propagation. We assumed that the inertial term in the dynamic equation is small with respect to the elastic and frictional forces. In the continuous limit, slip as a function of space and time obeys the same diffusion equation as temperature in 1D heat conduction (*22*). The problem of transient conduction in a 1D slab, when the temperature at one side is suddenly changed (slip begins) and the other side is kept at constant zero-temperature (no slip at the fault end), can be analytically resolved (*23*). The time evolution of the seismic moment (proportional to the integral of the slip over the fault) is given by the time evolution of the integral of the temperature and is very similar to the signals recorded by the interferometer (Figs. 1C and 5A). The seismic moment scales with fault width, and rise time scales with width squared. The seismic moment thus scales with the square root of rise time, in agreement with Fig. 4. Although the diffusion equation does not allow us to precisely define the velocity of the slip propagation, the point of maximum instantaneous slip-rate (Fig. 5B) propagates like the rupture in the decreasing velocity model used in (*4*) to fit the only event of the San Andreas sequence related to slow rupture propagation. If the model is realistic, the square root of time scaling would be a property of velocity-strengthening frictional systems in case the seismic moment time history is dominated by slip propagation.

References and Notes

1. I. S. Sacks, S. Suyehiro, A. T. Linde, J. A. Snoke, *Nature* **275**, 599 (1978).
2. M. T. Gladwin, R. L. Gwyther, R. H. G. Hart, K. Breckenridge, *J. Geophys. Res.* **99**, 4559 (1994).
3. I. Kawasaki *et al.*, *J. Phys. Earth* **43**, 105 (1995).
4. A. T. Linde, M. T. Gladwin, M. J. S. Johnston, R. L. Gwyther, R. G. Bilham, *Nature* **383**, 65 (1996).
5. H. Kanamori and E. Hauksson, *Bull. Seismol. Soc. Am.* **82**, 2087 (1992).
6. T. H. Jordan, *Geophys. Res. Lett.* **18**, 2019 (1991).
7. P. F. Ihmlé, P. Harabaglia, T. H. Jordan, *Science* **261**, 177 (1993).
8. P. F. Ihmlé and T. H. Jordan, *Science* **266**, 1547 (1994).
9. J. J. McGuire, P. F. Ihmlé, T. H. Jordan, *Science* **274**, 82 (1996).
10. S. Kedar, S. Watada, T. Tanimoto, *J. Geophys. Res.* **99**, 17893 (1994).
11. The nominal sensitivity of our interferometer is about 3×10^{-12} and its response time is of the order of milliseconds. During the transit of teleseismic waves, it recorded signals as large as 6×10^{-7} and as fast as 10^{-7} s^{-1} without any nonlinearity or abnormal behavior [L. Crescentini, A. Amoruso, G. Fiocco, G. Visconti, *Rev. Sci. Instrum.* **68**, 3206 (1997)].
12. Any interferometer measures the difference in extension between two baselines. From May 1994 to October 1995, we monitored the extension of a 90-m-long baseline (azimuth = N66E) approximately perpendicular to the Apennines, using a 20-cm-long reference baseline (azimuth = N24W). Because laser frequency fluctuations can give spurious signals whose amplitude depends on the difference in length between the two baselines, from December 1995 onward, both baselines were 90 m long and one component of shear strain was measured. Sampling rate was variable until 31 January 1996 and was fixed at 0.5 Hz since then. To avoid ambiguities due to the uneven sampling rate, we discuss data recorded from 1 February 1996 until 9 September 1997, when a power failure stopped data acquisition for a few weeks. However, data recorded before 31 January 1996 do not show any evidence of false signals similar to those discussed above.
13. A. Amoruso, L. Crescentini, R. Scarpa, *Geophys. J. Int.*, in press.
14. K. Kasahara, *Earthquake Mechanics* (Cambridge Univ. Press, Cambridge, 1981), pp. 28–37.
15. The central Apennines are characterized by spatially clustered seismic events; most of these relate to normal faults, oriented parallel with the Apennines (about N35W) and dipping toward the southwest at moderate angles of 40° to 70° [A. Amoruso, L. Crescentini, R. Scarpa, *J. Geophys. Res.* **103**, 29989 (1998); A. Amato *et al.*, *Geophys. Res. Lett.* **25**, 2861 (1998)].
16. Y. Okada, *Bull. Seismol. Soc. Am.* **75**, 1135 (1985).
17. M. Caputo, P. Gasperini, V. Keilis Borok, L. Marcelli, I. Rotwai, *Ann. Geophys.* **130**, 125 (1977); R. Scarpa and A. Zollo, *Earth. Predict. Res.* **1**, 81 (1985); E. Mantovani, D. Albarello, M. Mucciarelli, *Phys. Earth Planet. Inter.* **44**, 264 (1986); G. De Natale, F. Musmeci, A. Zollo, *Geophys. J.* **95**, 285 (1988); W. Marzocchi and F. Mulargia, *Geophys. Res. Lett.* **22**, 29 (1995).
18. D. P. Hill *et al.*, *Science* **260**, 1617 (1993).
19. Seismic moment is proportional to fault slip, length, and width. In the case of small earthquakes, slip and width usually scale with the fault length L (fixed stress-drop and geometric similarity) so that $M_0 \propto L^3 \propto \tau^3$. This last scaling law holds if one assumes that rupture propagates at constant velocity. In the case of large earthquakes, the fault width is independent of the earthquake size, so $M_0 \propto L^2 \propto \tau^2$ or maybe even $M_0 \propto L \propto \tau$ if slip scales with fault width [B. Romanowicz and J. B. Rundle, *Bull. Seismol. Soc. Am.* **83**, 1294 (1993)].
20. There is no general agreement about slow earthquake dynamics. According to some authors, they are not expected from the friction laws as currently formulated [C. H. Scholz, *Nature* **391**, 37 (1998)], while according to others, they are predicted by rate-state laws, under somewhat specialized rheologic properties [C. Marone, *Annu. Rev. Earth Planet. Sci.* **26**, 643 (1998)].
21. I. S. Sacks, A. T. Linde, J. A. Snoke, S. Suyehiro, in *Earthquake Prediction, An International Review*, D. W. Simpson and P. G. Richards, Eds. (Maurice Ewing Series 4, American Geophysical Union, Washington, DC, 1981), pp. 617–628; I. S. Sacks, S. Suyehiro, A. T. Linde, J. A. Snoke, *Tectonophysics* **81**, 311 (1982).
22. Each block of mass m is connected to its two neighbors with springs of stiffness k. Blocks move along the x-direction, and we designate the displacement of a particular block by y_i. Slipping is resisted by the dynamic friction $\beta dy_i/dt$. The motion of a single slipping block is given by

$$m\frac{d^2y_i}{dt^2} = -\beta\frac{dy_i}{dt} + k(y_{i+1} - 2y_i + y_{i-1}) \quad (1)$$

We assume the acceleration (inertial) term to be negligible with respect to the others. The remaining terms are the finite-difference approximation of the ordinary differential equation

$$-\frac{\partial y(x,t)}{\partial t} + \alpha\frac{\partial^2 y(x,t)}{\partial x^2} = 0 \quad (2)$$

Heat diffusion obeys the same equation, which is usually rearranged into nondimensional form by introducing the nondimensional length x/L and the nondimensional time $\alpha t/L^2$. Here, L is the characteristic length of the process.
23. The problem, with different boundary conditions, is discussed in J. H. Lienhard, *A Heat Transfer Textbook* (Prentice-Hall, Englewood Cliffs, NJ, 1981), pp. 152–155.

24. We thank M. R. Carroll, R. L. Gwyther, A. T. Linde, R. Madariaga, J. J. McGuire, and I. S. Sacks for helpful suggestions, and B. Farina for help in screening data. We are also grateful to E. Boschi (president, Istituto Nazionale di Geofisica) for authorizing the use of seismic data and to A. Bettini (director, LNGS) for the logistic support.

26 July 1999; accepted 27 October 1999

Possible Ancient Oceans on Mars: Evidence from Mars Orbiter Laser Altimeter Data

James W. Head III,[1]* Harald Hiesinger,[1] Mikhail A. Ivanov,[1,2] Mikhail A. Kreslavsky,[1,3] Stephen Pratt,[1] Bradley J. Thomson[1]

High-resolution altimetric data define the detailed topography of the northern lowlands of Mars, and a range of data is consistent with the hypothesis that a lowland-encircling geologic contact represents the ancient shoreline of a large standing body of water present in middle Mars history. The contact altitude is close to an equipotential line, the topography is smoother at all scales below the contact than above it, the volume enclosed by this contact is within the range of estimates of available water on Mars, and a series of extensive terraces parallel the contact in many places.

The northern lowlands occupy about one-third of the surface area of Mars (Fig. 1) and have played an important role in its hydrologic and climatic history (*1*). Large outflow channels empty into the northern lowlands (*2*), and a variety of distinctive morphologic features and geologic units occur there (*3–5*). Some investigators have hypothesized that large standing bodies of water, ranging in scale from lakes (*6*) to oceans (*7–10*), may have existed there in past Mars history. High-resolution altimetry data from the Mars Orbiter Laser Altimeter (MOLA) instrument on the Mars Global Surveyor (MGS) mission have underlined the un-

[1]Department of Geological Sciences, Brown University, Providence, RI 02912, USA. [2]Vernadsky Institute, Russian Academy of Sciences, Kosygina 19, 117975, Moscow, Russia. [3]Kharkov Astronomical Observatory, Kharkov University, Sumska 35, 310022, Kharkov, Ukraine.

*To whom correspondence should be addressed.

usual flatness and smoothness of the northern lowlands (*11*–*14*), have shown that they are part of the largest watershed on the planet (a drainage basin constituting three-quarters of the surface area of Mars) (*15*), and have permitted us to begin to test hypotheses for the presence of past standing bodies of water (*16*).

Parker *et al.* (*7*, *8*) mapped two contacts near and generally parallel to the southern boundary of the northern lowlands and interpreted these contacts to be shorelines, representing two separate highstands of a northern polar ocean. If the mapped contacts are ancient shorelines, then they should also represent the edge of a level surface and thus an equipotential line. If no vertical movement has occurred subsequent to their formation, the elevation of each contact should fall on a straight line when plotted as a function of longitude (Fig. 2). Plotting the elevation along 1136 orbits as they cross contact 1, we found that contact 1, with a mean elevation of −1680 m, is not a good approximation of an equipotential surface; variation in elevation shows highs in Tharsis, lows in Arabia, and ranges over almost 11 km (standard deviation = 1.7 km), an amount exceeding plausible values of postformation vertical movement. Contact 2, with 1191 orbit crossings, is a closer approximation to a straight line; the elevation range is ~4.7 km, with a mean value of −3760 m and a standard deviation of 560 m. The most substantial variations occur in Elysium and Arabia, where post–contact 2 activity has occurred (*17*), and in Tharsis, an area in which possible regional uplift has occurred (*18*). The variation in these three areas accounts for about 75% of the variability of the population of points at contact 2. Consideration of the influence of the presence of Tharsis on the geoid (*19*) would further reduce the scatter seen in the elevation of contact 2. We conclude that of the two contacts mapped by Parker *et al.* (*7*, *8*), contact 2 is the closest approximation to an equipotential line; the majority of the observed deviation from a straight line could plausibly be due to postformation modification and vertical movement.

Parker *et al.* (*7*, *8*) hypothesized that formation of an ocean would be accompanied by sedimentation, smoothing submarine terrain below the shoreline. The northern lowlands are flat and smooth relative to the rest of the planet (*11*–*14*), and MOLA data show that the average surface below contact 2 is smoother at all scales (from a few hundred meters to several tens of kilometers) than the surface between contacts 1 and 2 and that the surface is rougher at all scales above contact 1 than below.

Other workers have mapped geologic features thought to have been associated with the presence of bodies of water or residual ground ice, and the topographic data can be used to assess their locations. Lucchitta *et al.* (*20*) used Viking image data to identify the location and characteristics of possible sedimentary deposits in the northern lowlands (*21*). We digitized the map of the distribution of polygonally fractured terrain on Mars compiled by Lucchitta *et al.* (their Fig. 3) and superposed it on the MOLA topographic map (Fig. 3A); we found a correlation between the location of the polygonal ground and the deeper regions of the Utopia and North Polar basins within the northern lowlands, consistent with formation in areas formerly occupied by standing bodies of water (*7*, *8*).

Martian impact craters in the 2- to 50-km-diameter range commonly have ejecta deposits with distinctive lobe and rampart morphology, interpreted to be due to the presence of groundwater or ground ice in the target area that mobilizes the ejecta material (*22*). Craters on Mars smaller than a few kilometers generally do not have unusual ejecta ramparts, and thus the onset diameter of ramparts may be an indication of the depth at which groundwater or ground ice is encountered during cavity excavation. On the basis of this concept, Kuzmin *et al.* (*23*) assessed the onset diameter globally. Using their map, we found a correlation between the lower range of onset diameters (<4 km) and the northern lowlands (Fig. 3B). The craters with the smallest diameters (<2 km) correlate with the position of the two large basins within the northern lowlands, a distribution consistent with an interpretation of groundwater or ground ice occurring preferentially near the surface in the northern lowlands and particularly in the interiors of the two basins (*7*, *8*).

Assuming that the present topography is a reasonable approximation of the topography in the geological past, we found that the total volume represented by the topography below contact 2 is about 1.4×10^7 km^3 and about 10% more if the polar cap (*13*) is absent. These volumes lie between the minimum estimates of the volume that flowed through the Chryse outflow channels (about 0.6×10^7 km^3) (*1*) and the maximum value of 5 to 20×10^7 km^3 for megaregolith pore space that might potentially contain water (*3*). The volume contained by contact 2, equivalent to a global layer almost 100 m deep, lies within the range of estimates of available water (*1*).

The northern hemisphere topographic map permits us to assess what would happen if (i) individual channels emptied into the lowlands at different times and proceeded to fill them (*7*–*9*), (ii) the lowlands were flooded by a different mechanism (as in the case of an ancient ocean older than the outflow channels) (*10*), and (iii) a putative ocean began to recede. We sequentially flooded the northern lowlands and observed where water would pond and how candidate oceans might evolve with changing depth (Fig. 3, C to F). These maps show two distinctive

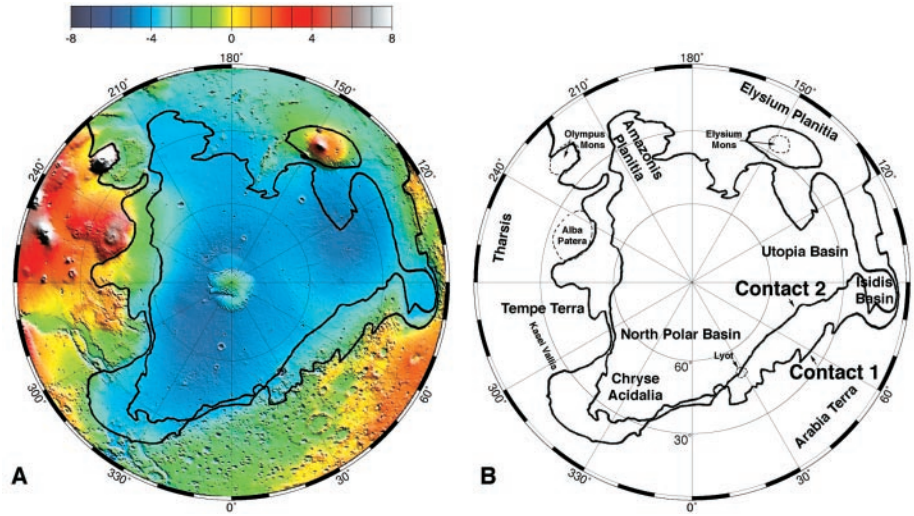

Fig. 1 (top). (**A**) Lambert equal-area projection of MOLA North Pole–to-equator topography (*15*). Black lines indicate positions of contacts interpreted to be shorelines (*7*, *8*). Elevation is given in kilometers. (**B**) Major features described in the text.

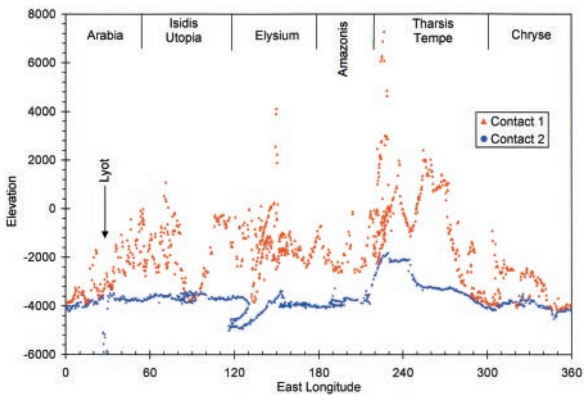

Fig. 2 (bottom). Elevation (in meters) of contacts 1 and 2 as a function of longitude (in degrees). Data are through orbit 10464, 15 April 1999 (revision d).

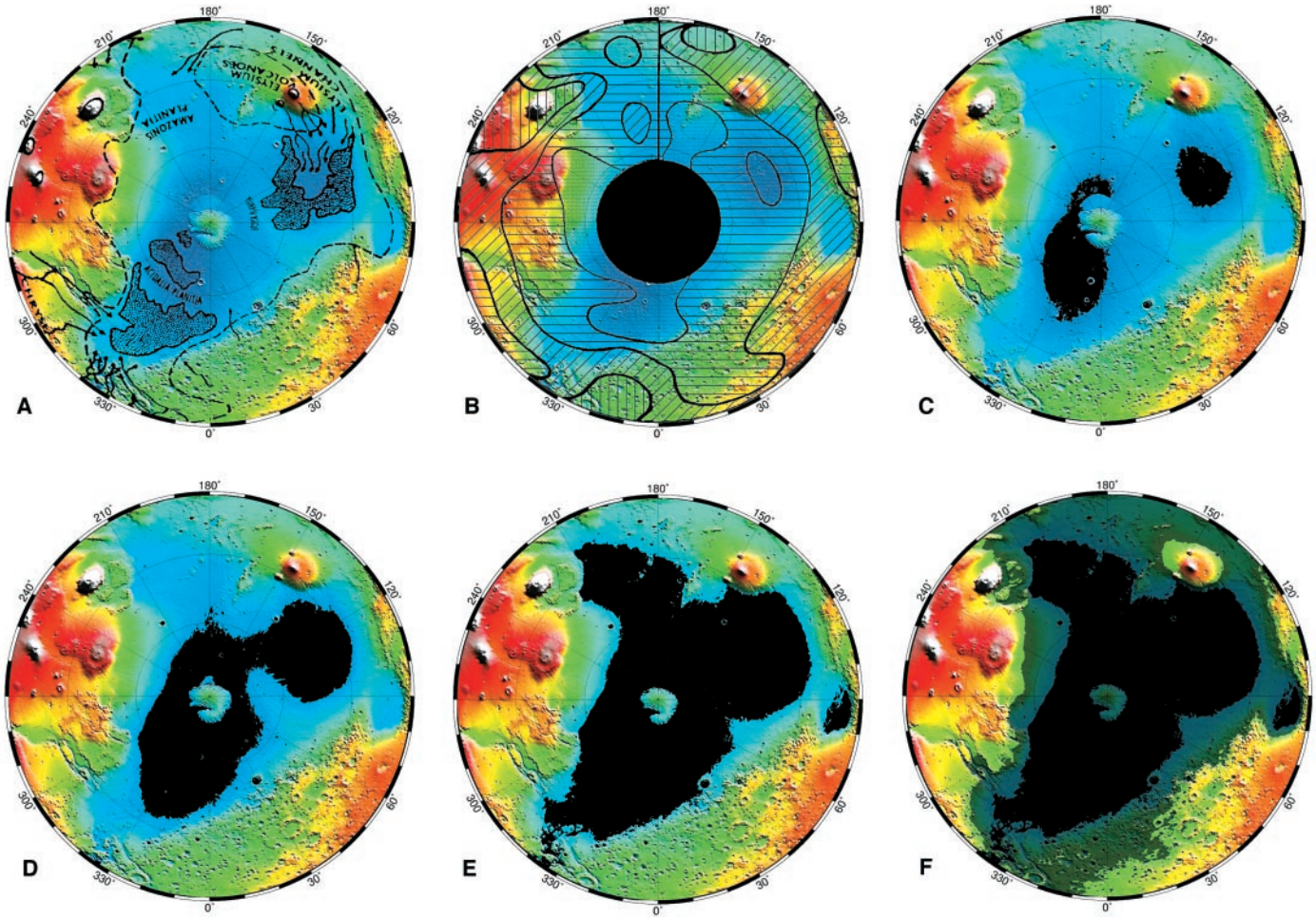

Fig. 3. (**A**) Distribution of polygons (stippled areas) (*20*). Dashed lines indicate the northern edge of the highlands. (**B**) Distribution of onset diameter of impact craters with ejecta lobes (*23*). Diameters are as follows: dotted area, 0 to 2 km; horizontal hatching, 2 to 4 km; diagonal hatching, 4 to 6 km; and vertical hatching, 6 to 8 km. Black central area was not analyzed by (*23*). (**C** to **F**) Sequential flooding (black areas) of the northern lowlands. Flooded to a total depth of (C) 500 m, (D) 1000 m, (E) 1490 m (level of contact 2), and (F) the mean level of contact 1 (−1680 m), with level of contact 2 shown underneath.

basins in the northern lowlands, the circular Utopia basin of probable ancient impact origin (*24*) and the irregularly shaped North Polar basin (Fig. 3C). The lowest topography in the northern lowlands occurs in the North Polar basin (~−5250 m). Starting at this elevation, as much as 5.4×10^4 km^3 of water might accumulate there before the initiation of filling of the Utopia basin. At a maximum water depth of 500 m, both basins would contain water (Fig. 3C); at a maximum water depth of 1000 m (Fig. 3D), the basins would become interconnected through a narrow topographic trough, and each basin would contain in excess of 10^6 km^3. Continued filling to the approximate level of contact 2 (about −3760 m) (Fig. 3E) yields a volume of ~1.4×10^7 km^3 and an average depth of ~560 m. Filling to the mean level of contact 1 (about −1680 m) yields ~9.6×10^7 km^3 in the northern hemisphere (Fig. 3F).

Outflow channels emptying into the northern lowlands from Chryse and Amazonis would flow into the North Polar basin, whereas channels originating in western Elysium would empty into the Utopia basin. Total amounts of water for individual outflow channel floods are poorly constrained (*1*, *9*). Carr estimated that water volumes for individual channels might range up to ~3×10^5 km^3 (*1*). Such a channel event could have filled the North Polar basin to about −4900 m (a maximum depth of ~350 m; 120 m average), and it would take at least eight to nine such channel events to fill the basin before it overflowed into the Utopia basin. At least 40 events would be required to fill the northern lowlands to the level of contact 2. Outflow channel formation occurred over an extended period of time (*2*, *25*, *26*), and it seems likely that at least some of the water emplaced in the northern lowlands by each event would disappear between events (*9*). If a shoreline corresponding to the position of contact 2 (*7*, *8*) originated solely through the cumulative emplacement of Hesperian/Amazonian-aged outflow channel events, very high volumes, multiple discharge events through each channel, or a narrow range of emplacement times (or several of the above) would be required (*9*).

Other hypotheses suggest that large-scale standing bodies of water may have existed in the northern lowlands since the Noachian Period (*9*–*10*), before the formation of the Hesperian-aged outflow channels. If such an early ocean existed at the time of the emplacement of the outflow channels, then evidence for the interaction of the outflow channels and the ocean may exist. Noting that the distinctive landforms of the distal portions of outflow channels commonly end abruptly in the northern lowlands (*1*, *26*), we examined the elevations of the terminations of the six major outflow channels that empty into Chryse Planitia, reasoning that these elevations would be variable depending on such factors as discharge, age, subsequent events, and the level of a possible standing body of water (*7*, *8*) at the time of their emplacement. The elevations of the terminations of each of six channels differ by a maximum of 340 m, even though channels are separated by several hundred kilometers each and are spread over a total lateral distance of

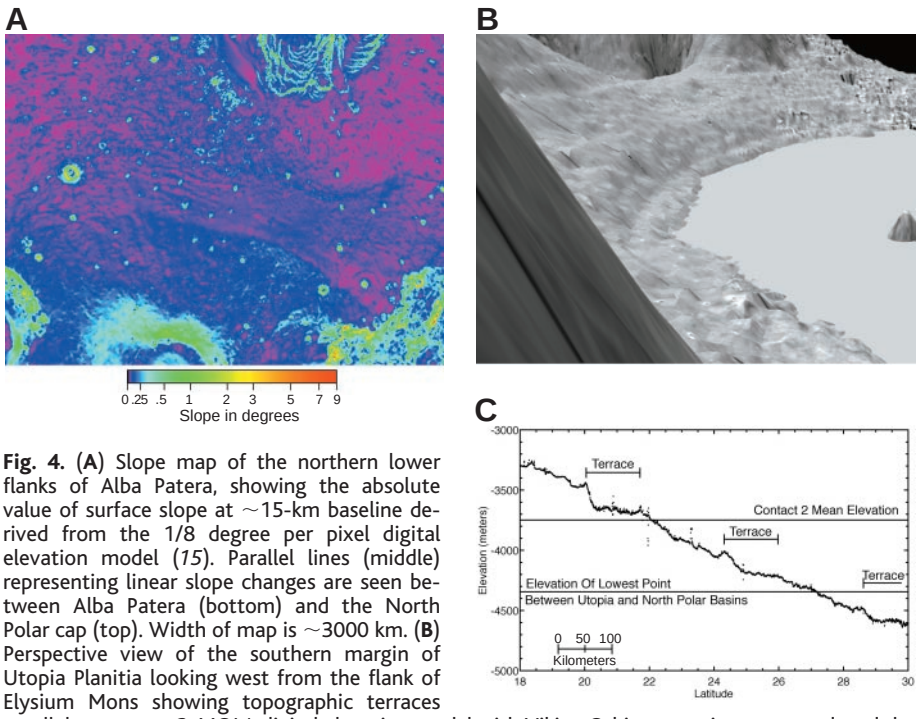

Fig. 4. (**A**) Slope map of the northern lower flanks of Alba Patera, showing the absolute value of surface slope at ~15-km baseline derived from the 1/8 degree per pixel digital elevation model (*15*). Parallel lines (middle) representing linear slope changes are seen between Alba Patera (bottom) and the North Polar cap (top). Width of map is ~3000 km. (**B**) Perspective view of the southern margin of Utopia Planitia looking west from the flank of Elysium Mons showing topographic terraces parallel to contact 2; MOLA digital elevation model with Viking Orbiter mosaic superposed, and the basin flooded to just below the −4350-m contour, the elevation where the Utopia and North Polar basins become interconnected. Vertical exaggeration is ~×200. (**C**) MOLA profile (10190) in southern Utopia Planitia.

2200 km. In addition, the mean elevation of all channel terminations lies within 60 m of the mean elevation of contact 2 (*27*). These observations suggest that a large standing body of water existed at about the position of contact 2 at the time of emplacement of the outflow channels; in this scenario, the abrupt termination of distinctive channel morphology is due to the channels debouching into an existing standing body of water and changing from a predominantly erosional regime to a predominantly depositional regime.

If recession of a standing body of water did indeed occur, one would predict that the margins of the body of water would approximately follow the reverse order of the filling sequence outlined in Fig. 3, C to E. If such a recession was nonlinear (for example, due to modulation by outflow channel events, climate change, or other factors), then evidence might exist for the position of regional "stillstands" in the form of changes in depositional environments, wave-cut terraces, or ice-margin processes if the body was frozen over. All of these processes could produce changes in slope at the position of the boundary, as is commonly seen in retreating bodies of water on Earth (*28*). We compiled regional slope maps of the northern lowlands and searched for evidence for slope changes arrayed in a linear fashion. We found distinctive linear slope changes within the Utopia basin and the North Polar basin (Fig. 4). These linear slope changes (Fig. 4A) extend for many tens of kilometers, parallel one another and topographic contours, occur near or below contact 2, and are faint or absent in the lowest parts of the Utopia and North Polar basins. Linear slope changes are most prominent along the lower northern flanks of Alba Patera (Fig. 4A) and along the southern margin of the Utopia basin (Fig. 4B) (*29*), although some occur around other margins of Utopia. Detailed assessment of individual profiles crossing these linear slope changes (Fig. 4C) shows that some of the most prominent ones in Utopia are near the position of contact 2 and the approximate elevation where the two basins would first become interconnected (*29*) (see Fig. 3D).

Other processes (volcanic, eolian, and glacial) have contributed to the shaping of the northern lowlands throughout its history as they have elsewhere on Mars. We found that no single alternative process, however, emerges as a dominant factor in the shaping of the northern lowlands or is as consistent with all of the observations as the presence of former standing bodies of water. We conclude that MOLA data used to test a large number of predictions are consistent with hypotheses calling on large standing bodies of water in the northern lowlands in the past history of Mars and that these hypotheses should be seriously considered and tested further (*30*). Among these tests should be further analysis and interpretation of data from martian meteorites and landing sites. Recent theories for the evolution of samples from Mars call on the presence of ancient bodies of water in their evolution (*31*). Viking 1 and 2 landed below contact 2 and Pathfinder landed near it (*32*), and some of the anomalous chemistry (for example, unusual abundances of S and Cl and their possible presence as sulfate minerals and chloride salts) (*33*) may be related to the presence of former standing bodies of water.

References and Notes

1. M. H. Carr, *Water on Mars* (Oxford Univ. Press, New York, 1996).
2. V. R. Baker *et al.*, in *Mars*, H. H. Kieffer, B. M. Jakosky, C. W. Snyder, M. S. Matthews, Eds. (Univ. of Arizona Press, Tucson, AZ, 1992), pp. 493–522.
3. S. W. Squyres *et al.*, in *Mars*, H. H. Kieffer, B. M. Jakosky, C. W. Snyder, M. S. Matthews, Eds. (Univ. of Arizona Press, Tucson, AZ, 1992), pp. 523–554.
4. P. Thomas *et al.*, in *Mars*, H. H. Kieffer, B. M. Jakosky, C. W. Snyder, M. S. Matthews, Eds. (Univ. of Arizona Press, Tucson, AZ, 1992), pp. 767–795.
5. K. L. Tanaka and D. H. Scott, *U.S. Geol. Surv. Misc. Invest. Ser. Map I-1802-C* (1987).
6. D. H. Scott *et al.*, *U.S. Geol. Surv. Misc. Invest. Ser. Map I-2461* (1995); D. H. Scott *et al.*, *Proc. Lunar Planet. Sci.* **22**, 53 (1992).
7. T. J. Parker *et al.*, *Icarus* **82**, 111 (1989).
8. T. J. Parker *et al.*, *J. Geophys. Res.* **98**, 11061 (1993).
9. V. R. Baker *et al.*, *Nature* **352**, 589 (1991).
10. S. Clifford and T. J. Parker, *Lunar Planet. Sci. Conf.* **30**, 1619 (1999).
11. D. E. Smith *et al.*, *Science* **279**, 1686 (1998).
12. O. Aharonson, *Geophys. Res. Lett.* **25**, 4413 (1998); M. A. Kreslavsky and J. W. Head, *J. Geophys. Res.* **104**, 21911 (1999).
13. M. T. Zuber *et al.*, *Science* **282**, 2053 (1998).
14. J. Garvin *et al.*, *Geophys. Res. Lett.* **26**, 381 (1999).
15. D. E. Smith *et al.*, *Science* **284**, 1495 (1999).
16. J. W. Head *et al.*, *Geophys. Res. Lett.* **25**, 4401 (1998).
17. R. Greeley and J. E. Guest, *U.S. Geol. Surv. Misc. Invest. Ser. Map I-1802-B* (1987); D. H. Scott and K. L. Tanaka, *U.S. Geol. Surv. Misc. Invest. Ser. Map I-1802-A* (1986); K. L. Tanaka *et al.*, *U.S. Geol. Surv. Misc. Invest. Ser. Map I-2147* (1992).
18. W. B. Banerdt *et al.*, in *Mars*, H. H. Kieffer, B. M. Jakosky, C. W. Snyder, M. S. Matthews, Eds. (Univ. of Arizona Press, Tucson, AZ, 1992), pp. 249–297.
19. M. T. Zuber and D. E. Smith, *J. Geophys. Res.* **102**, 28673 (1997).
20. B. K. Lucchitta *et al.*, *J. Geophys. Res.* **91** (suppl. B13), 166 (1986).
21. G. E. McGill, *Geophys. Res. Lett.* **13**, 705 (1986).
22. M. H. Carr *et al.*, *J. Geophys. Res.* **82**, 4055 (1977).
23. R. Kuzmin *et al.*, *Solar Syst. Res.* **22**, 195 (1988).
24. G. E. McGill, *J. Geophys. Res.* **94**, 2753 (1989).
25. H. Masursky *et al.*, *J. Geophys. Res.* **82**, 4016 (1977).
26. S. Rotto and K. L. Tanaka, *U.S. Geol. Surv. Misc. Invest. Ser. Map I-2441* (1995); K. L. Tanaka, *J. Geophys. Res.* **102**, 4131 (1997).
27. M. A. Ivanov and J. W. Head, in *Fifth International Conference on Mars* (Lunar and Planetary Institute, Houston, TX, 1999), abstract 6176 [CD-ROM].
28. E. C. Bird, *Coasts* (MIT Press, Cambridge, MA, 1969); P. D. Komar, *Beach Processes and Sedimentation* (Prentice-Hall, Englewood Cliffs, NJ, 1976).
29. B. J. Thomson and J. W. Head, *Lunar Planet. Sci. Conf.* **30**, 1894 (1999).
30. M. Malin and K. Edgett, *Geophys. Res. Lett.* **26**, 3049 (1999).
31. H. Y. McSween, *Int. Geol. Rev.* **40**, 774 (1998); P. Warren, *J. Geophys. Res.* **103**, 16759 (1998).
32. T. A. Mutch *et al.*, *Science* **193**, 791 (1976); T. A. Mutch *et al.*, *Science* **194**, 1277 (1976); M. Golombek *et al.*, *Science* **278**, 1743 (1997).
33. A. Banin *et al.*, in *Mars*, H. H. Kieffer, B. M. Jakosky, C. W. Snyder, M. S. Matthews, Eds. (Univ. of Arizona Press, Tucson, AZ, 1992), pp. 594–625; H. Y. McSween *et al.*, *J. Geophys. Res.* **104**, 8679 (1999).

34. We gratefully acknowledge the MOLA instrument team and the MGS spacecraft and operation teams at the Jet Propulsion Laboratory and Lockheed-Martin Astronautics for providing the engineering foundation that enabled this analysis. This effort was supported by MOLA (NASA Mars Global Surveyor Project) and NASA grant NAG5-8283.

8 September 1999; accepted 4 November 1999